



LAWRENCE
LIVERMORE
NATIONAL
LABORATORY

Diagnostics for Fast Ignition Science

A.G. MacPhee, K. Akli, F.N. Beg, C.D. Chen, H. Chen, R. Clarke, D. Hey, R.R. Freeman, A.J. Kemp, M.H. Key, J.A. King, S. LePape, A. Link, T. Ma, N. Nakamura, D.T. Offermann, V.M. Ovchinnikov, P.K. Patel, T.W. Phillips, R.B. Stephens, R. Town, M. Wei, L.D. VanWoerkom, A.J. Mackinnon

May 7, 2008

High Temperature Plasma Diagnostics
Albuquerque, NM, United States
May 11, 2008 through May 15, 2008

Disclaimer

This document was prepared as an account of work sponsored by an agency of the United States government. Neither the United States government nor Lawrence Livermore National Security, LLC, nor any of their employees makes any warranty, expressed or implied, or assumes any legal liability or responsibility for the accuracy, completeness, or usefulness of any information, apparatus, product, or process disclosed, or represents that its use would not infringe privately owned rights. Reference herein to any specific commercial product, process, or service by trade name, trademark, manufacturer, or otherwise does not necessarily constitute or imply its endorsement, recommendation, or favoring by the United States government or Lawrence Livermore National Security, LLC. The views and opinions of authors expressed herein do not necessarily state or reflect those of the United States government or Lawrence Livermore National Security, LLC, and shall not be used for advertising or product endorsement purposes.

Diagnostics for Fast Ignition Science

A. G. MacPhee¹, K. U. Akli², F. N. Beg³, C. D. Chen¹, H. Chen¹, R. Clarke⁴, D. S. Hey¹, R. R. Freeman⁵,
A. J. Kemp¹, M. H. Key¹, J. A. King³, S. Le Pape¹, A. Link⁵, T. Y. Ma³, H. Nakamura⁶, D. T. Offermann⁵,
V. M. Ovchinnikov⁵, P. K. Patel¹, T. W. Phillips¹, R. B. Stephens², R. Town¹, M. S. Wei³, L. D. Van
Woerkom⁵, A. J. Mackinnon¹

¹*Lawrence Livermore National Laboratory, Livermore, CA*

²*General Atomics, San Diego, CA*

³*Department of Mechanical and Aerospace Engineering, University of California-San Diego, La Jolla, CA*

⁴*CCLRC Rutherford Appleton Laboratory, Oxfordshire, UK*

⁵*College of Mathematical and Physical Sciences, The Ohio State University, Columbus, OH*

Institute of Laser Engineering, Osaka University, Suita, Osaka, Japan

(925) 422 3720, macphee2@llnl.gov

Abstract

The concept for Electron Fast Ignition Inertial Confinement Fusion demands sufficient laser energy be transferred from the ignitor pulse to the assembled fuel core via ~MeV electrons. We have assembled a suite of diagnostics to characterize such transfer. Recent experiments have simultaneously fielded absolutely calibrated extreme ultraviolet multilayer imagers at 68 and 256eV; spherically bent crystal imagers at 4 and 8keV; multi-keV crystal spectrometers; MeV x-ray bremsstrahlung and electron and proton spectrometers (along the same line of sight); nuclear activation samples and a picosecond optical probe based interferometer. These diagnostics allow careful measurement of energy transport and deposition during and following laser-plasma interactions at extremely high intensities in both planar and conical targets. Augmented with accurate on-shot laser focal spot and pre-pulse characterization, these measurements are yielding new insight into energy coupling and are providing critical data for validating numerical PIC and hybrid PIC simulation codes in an area that is crucial for many applications, particularly fast ignition. Novel aspects of these diagnostics and how they are combined to extract quantitative data on ultra high intensity laser plasma interactions are discussed, together with implications for full-scale fast ignition experiments.

Introduction

Fast ignition (FI) is a relatively new concept that decouples the compression and ignition stage in inertial confinement. This concept has the potential to provide a significant advance in the technical attractiveness of Inertial Fusion Energy (IFE) reactors. FI differs from conventional “central hot spot” (CHS) target ignition by using one driver (laser, heavy ion beam or Z-pinch) to create a dense fuel and a separate ultra-short, ultra-intense laser beam to ignite the dense core. FI targets can burn with $\sim 3X$ lower density fuel than CHS targets, resulting in lower required compression energy, relaxed drive symmetry, relaxed target smoothness tolerances, and, importantly for IFE and ignition applications, higher gain. The short, intense ignition pulse that drives this process interacts with extremely high energy density plasmas; the physics that controls this interaction is only now becoming accessible in laboratory experiments through the advent of multiple energetic short pulse lasers and the development of novel diagnostics that allows accurate and in situ probing of energy deposition and transport in metals and hot plasmas. Present designs for fast ignition use a hollow Au cone inserted in the spherical shell as illustrated

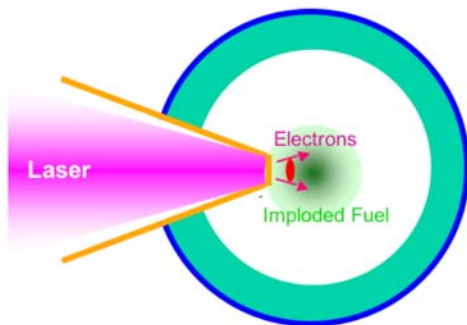


Figure 1 Schematic of the cone in shell concept first proposed for fast ignition

in Fig. 1. The fuel compression implosion produces the dense compressed fuel plasma at the tip of the cone, while the hollow cone permits the short-pulse ignition laser to be transported to the dense fuel without interference, and enables the generation of hot electrons at its tip, very close to the dense

plasma.

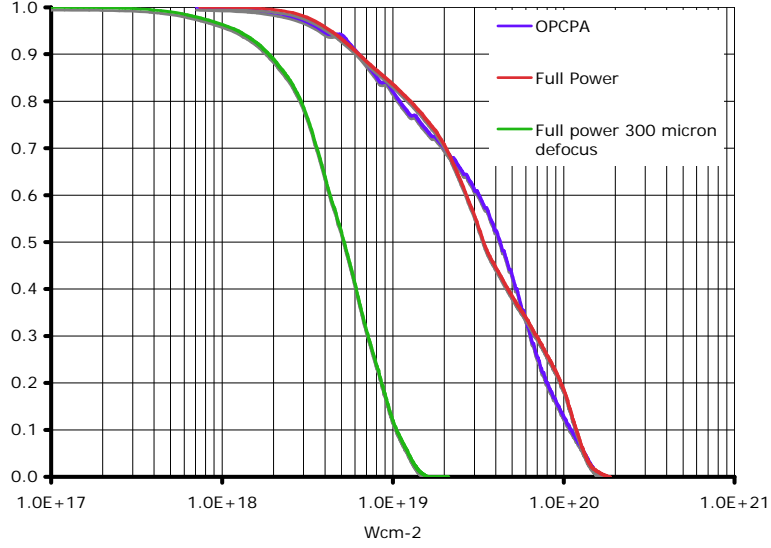
The critical unresolved issue is the physics of the dynamics of the current propagation from the critical density near the cone tip into the assembled fuel. The requirements on the short pulse laser have been determined from hydrodynamic and burn calculations as described by Tabak and Atzeni et al.,^{1, 2}. These articles describe the required energy, pulselength, heated volume size and particle range required for successful ignition of compressed Deuterium-Tritium (DT) targets. The minimum requirements (for compressed fuel of density 500g/cc and $\rho R = 2\text{g/cm}^{-2}$) are hot electron total energy, $E_h = 18\text{kJ}$, electron beam pulselength, $T_p = 10\text{ps}$, electron beam radius, $r_{\text{beam}} = 40\mu\text{m}$ and mean particle range of 2gcm^{-2} (equivalent to 2MeV electrons). Assuming a conversion efficiency from laser to (1-2MeV) electrons of 30%^{3,4} results in a required focused laser irradiance at the cone tip of $5 \times 10^{20} \text{ Wcm}^{-2}$. According to the ponderomotive scaling⁵ this laser intensity would result in an electron distribution with a mean temperature of 5-7MeV. This is not well matched to the column density of the fuel and results in inefficient coupling of laser to target, which subsequently increasing the energy required to ignite the target. However the validity of ponderomotive scaling has not been adequately tested with laser conditions above $1 \times 10^{19} \text{ Wcm}^{-2}$ and there is some theoretical work that suggests that profile steepening by the light pressure can result in lower hot electron energy⁶. There is a clear need to measure both absolute conversion efficiency and hot electron energy distribution as a function of laser intensity in $1 \times 10^{20} \text{ Wcm}^{-2}$ regime. Once validated, these measurements will be used to benchmark integrated codes that will in turn be used to design integrated fast ignition (FI) experiments^{7,1,8} on large scale facilities such as Omega EP, NIF ARC and Firex. The key parameters of interest

are conversion efficiency from laser energy to hot electrons and the associated electron spectrum. An accurate knowledge of the laser pre-pulse profile, the subsequent pre-formed plasma profile, and the laser focal spot intensity distribution is required to reliably determine the specifications of the experimental parameters required for these integrated experiments. In this article we describe recent techniques designed to carry out these measurements. These will be compared and contrasted to conventional electron spectrum measurements obtained simultaneously using vacuum electron spectrometers.

II Diagnostics required for Fast Ignition experiments

II.1 Laser diagnostics

In order to accurately model the electron source produced by the laser matter interaction the laser intensity, the prepulse conditions and the resulting preformed plasma conditions must be measured on every shot. On the experiments described here the laser power is monitored by measuring the on-shot energy using a calorimeter, and pulselength using an autocorrelator or single shot grenouille ⁹. This gives a power measurement within a shot to shot accuracy of 20%. The intensity distribution at the target plane is optimized with an in-situ microscope using a 16-bit CCD camera monitoring the heavily attenuated pulsed alignment beam. The on shot intensity distribution at the target plane is measured using an equivalent plane monitor (EPM) that records the focal spot from a full aperture 6.4m f/26 lens collecting 10^{-5} leakage through the final turning mirror prior to the final f/3 focusing optic. The image is recorded on a 16-bit ccd via an infinity corrected microscope. This design permits interchanging filters depending on shot parameters without compromising alignment. The EPM characterizes the effects of pump induced



distortion and non linear optical refractive index on the full power focal spot. To preserve Fresnel zone number for defocused shots the location of the equivalent focal plane in the EPM scales as the square of the focal ratio of the two optics ($\Rightarrow (6320/750)^2 = 70.56$). The low transmission of the final turning mirror ensures that there are no B-integral effects in the EPM system that might cause an increase in the measured focal spot. The experimental set up and typical results are shown in figure 2(a) and (b) respectively. It can be seen from Fig (2 (b) that the intensity distribution does not change between the pulsed alignment beam and full system shots. ($\sim \mu\text{J}$ vs $\sim 150\text{J}$). Peak on shot intensity is thus demonstrated to be in excess of $1 \times 10^{20} \text{ Wcm}^{-2}$.

The on-shot pre-pulse is measured on every shot using a diode and water cell system as shown next to the EPM in fig 2a. This system is capable of measuring the pulse shape up to 100ps before the peak of the pulse and has been used to measure the few nanosecond super fluorescence and low energy replicas of the main pulse caused by

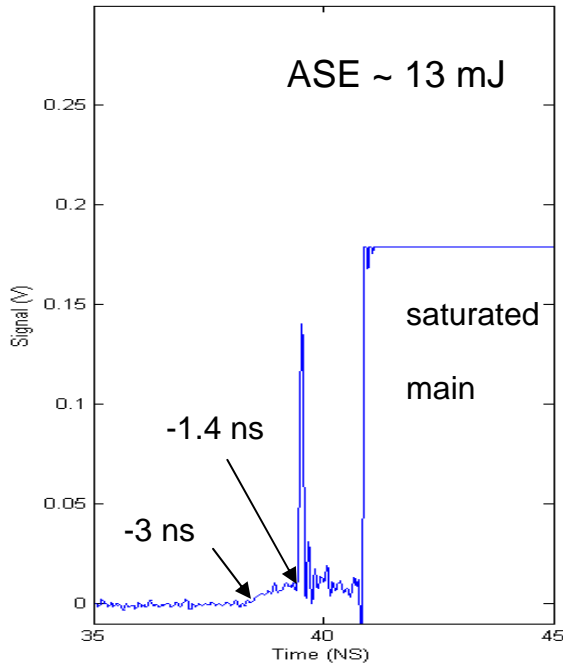


Figure 2 Typical trace from pre-pulse monitor

ows a typical trace of the laser pulse on a the typical features that are important for iced by this pulse. There is a slowly rising ak of main pulse followed by a very short ain pulse. This system has shown that the se of 1-10mJ, partitioned between the se features are important for determining ts are described in more detail in a gether the EPM and prepulse monitor are ing conditions for the models used to i the next section.

II.2 Hot electron source size

Images of the K- α fluorescence are used to measure the hot electron source size. Two techniques are currently used, 2D imaging with spherically bent Bragg crystals to measure the hot electron source size in buried fluor layers and pinhole imaging using Ross pair filters and image plate detectors. Initial experiments concentrated on fluorescence from Ti and Cu fluors. However, the relatively low ionization cross sections of Ti and Cu can push the emission away from the Bragg peak of the crystal, resulting in a distorted image of the hot spot and an underestimate of the total K- α yield. For this reason and to reduce the effective opacity for fluorescence imaging in integrated experiments, we are shifting attention to higher Z fluors. For Zr we are evaluating spherically bent quartz (3140) in 3rd order¹⁰. Above Zr there are no suitable crystals for

efficient 2D imaging. For Ag we are evaluating a pinhole array imager with a Pd/Mo Ross pair filter to isolate the Ag K- α signal.

II.3 Hot electron energy distribution

The distribution of hot electrons and associated hot electron temperature T_{hot} is determined from the bremsstrahlung spectrum that escapes the target. Bremsstrahlung spectra for ultra intense laser plasma interactions extend to hundreds of keV and to measure them we use a differential Z filter stack spectrometer¹¹.adapted for petawatt scale interactions (figure 4a). The Monte Carlo model Integrated Tiger Series (ITS) is used to construct response matrices for both the target and the detector. For the target matrix an array of bremsstrahlung spectra are generated for a series of discrete electron

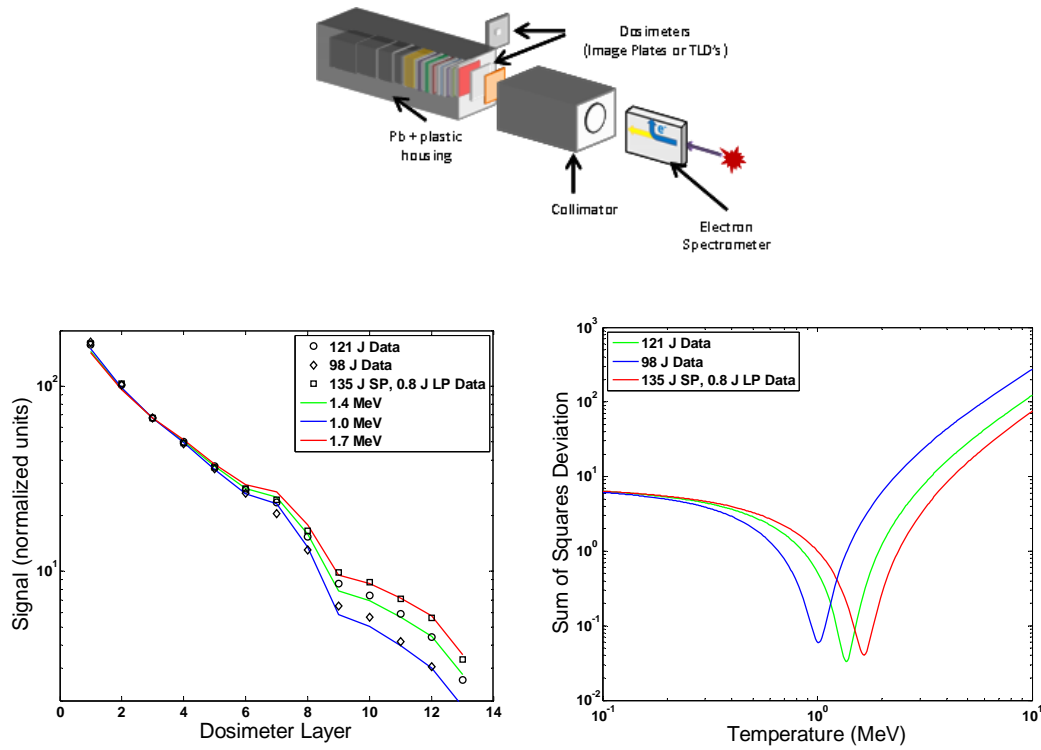


Figure 3a Bremsstrahlung spectrometer, 4b signal and best fit to signal, 4c T-hot fit error estimate

energies. For the detector matrix an array of dose per dosimeter is generated for a series of discrete X-ray energies. The electron energy distribution is varied to minimize the standard deviation in the resulting fit to the measured bremsstrahlung spectrum. Anything greater than a 1 temperature fit (figure 4b, 4c) requires additional constraints be placed on the model. Absolute calibration of the dosimeters, both image plates and thermo luminescent detectors is underway to achieve this and additional measurements using nuclear activation to extend the bremsstrahlung measurement out to several MeV are being pursued in an attempt to further constrain the model.

II.4 Laser to hot electron conversion efficiency

Hot electron conversion efficiency is inferred by measuring the K- α fluorescence induced in the target substrate⁴. Accurate measurements of absolute signal are obtained from

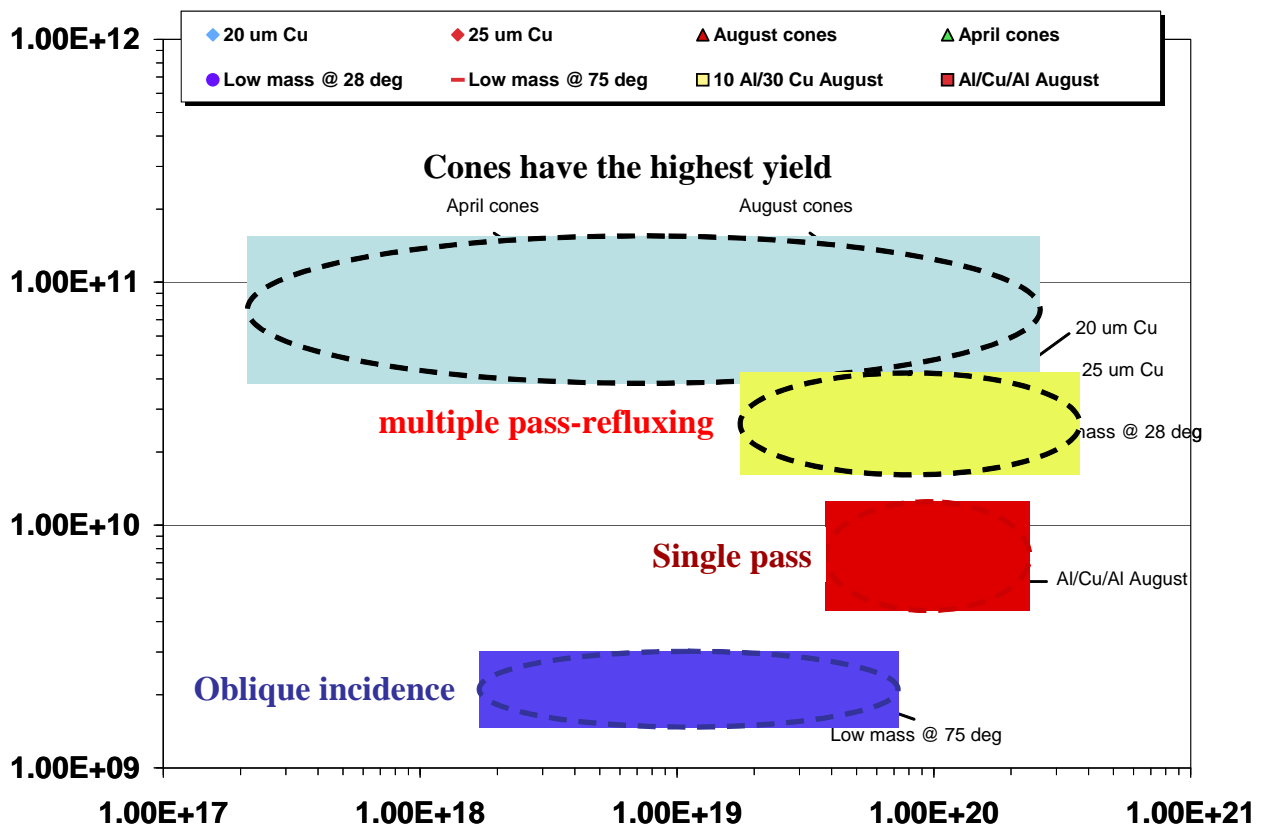


Figure 4 -alpha yield (photons per steradian per incident Joule) vs peak intensity on target for a range of target configurations

crystal spectra calibrated against an absolutely calibrated single hit CCD camera. To maintain linearity on the CCD, it is typically necessary to maintain a single hit count rate below $\sim 5\%$ of the total number of pixels, with $\sim 1\text{-}10\%$ of these attributed to K- α events. Good statistics for the calibration are obtained by summing over several shots. The conversion efficiency measurements shown in figure 5 illustrate the effect of electron refluxing and laser incidence angle on K- α production. The oblique incidence shots correspond to the same interaction angle experienced by cones of a similar mass, illustrating enhanced yield from a wall confined plasma.

Conclusion

The next generation of sub-scale integrated fast ignition experiments on the OMEGA EP, FIREX I, and NIF ARC laser facilities will require sophisticated target designs developed with well validated modeling tools. The most important parameters related to the ignition pulse are the mean hot electron energy and laser-to-electron conversion efficiency. Since direct measurements of the electrons at their source are not possible one must rely on indirect measurements, coupled with modeling to determine the quantities of interest. We have implemented a suite of diagnostics based on hot electron generated K-alpha x-ray and Bremsstrahlung emission measurements, which when combined serve to constrain the inferred hot electron distribution function and conversion efficiency. Benchmarking PIC and hybrid PIC calculations, as well as physical scaling laws, against experimental data additionally requires well characterised laser interaction parameters, including full energy focal spot intensity distributions and pre-pulse measurements. The techniques described herein using high energy x-rays to characterize the hot electron distribution can be applied to experiments on the next generation of multi-kiloJoule class short-pulse

lasers. Such experiments will be an essential pre-requisite for the design and optimization of fast ignition targets, and for the interpretation of measurements, such as neutron yields and K-alpha fluorescence, in integrated fast ignition experiments.

Acknowledgements

This work performed under the auspices of the U.S. Department of Energy by Lawrence Livermore National Laboratory under Contract DE-AC52-07NA27344

¹ M. Tabak, J. Hammer, M.E. Glinsky, *et al*, Phys. Plasmas **1**, 1626 (1994).

² S Atzeni, Physics of Plasmas **14**, 052702 (2007).

³ K. Yasuike, M. J. Key, S. P. Hatchett, R. A. Snavely, and K. B. Wharton, Rev. Sci. Instrum. **71**, 1236 (2001).

⁴ K. B. Wharton, S. P. Hatchet, S. C. Wilks et al., Phys. Rev. Lett. **81**, 822 (1998).

⁵ S. C. Wilks et al., Phys. Rev. Lett. **69**, 1383 (1992).

⁶ A. Kemp, Y. Sentoku, M. Tabak, Submitted to Phys. Rev. Lett.

⁷ N.G. Basov, S.Y. Guskov, L.P. Feokistov, J. Supercrit. Fluids **13**, 396 (1992).

⁸ M.H. Key, Phys. Plasmas, **14**, 055502 (2007).

⁹ P. O'Shea et al., Opt. Lett. **26**, 932 (2001); www.swampoptics.com

¹⁰ J.A. Koch, O.L. Landen, T.W. Barbee *et al.*, Appl. Opt. **37** (10), 1784 (1998).

¹¹ R. Nolte, R. Behrens, M. Schnürer, *et al.*, Radiat. Prot. Dosim. **84** (1-4), 367 (1999)